Journal of Ceramic Processing Research. Vol. 10, No. 3, pp. 401~407 (2009)

J O U R N A L O F
Ceramic Processing Research

Three-dimensional modelling and analysis of cross-flow filtration combustion

Sungyoung Mun[a], Yoo Taek Kim[b], Kwang Bo Shim[c] and Sung Chul Yi[a,d]*

[a]*Dept. of Chemical Engineering, Hanyang University, Seoul, Korea*
[b]*Dept. of Advanced Materials Engineering, Kyonggi University, Suwon, Korea*
[c]*Dept. of Advanced Materials Engineering, Hanyang University, Seoul, Korea*
[d]*Fuel Energy Research Institute, Hanyang University, Seoul, Korea*

Given that combustion synthesis reactions have a highly exothermic nature and a high activation energy, filtration combustion proceeds in the form of sharp fronts. Various front propagation phenomena are observed due, not only to the non-linear nature of the system, but also to the interaction of the gas-flow with the combustion front. In this study, a two-dimensional model of filtration combustion [1] in FLUENT using user-defined-functions (UDFs) was successfully expanded into a three dimensional model to study the behavior of the real systems. The implementation of the new three-dimensional model is validated using a sample problem solved earlier by Degreve *et al.* [2] and the new model correctly captures the complex behavior of the combustion front.

Key words: Filtration combustion, FLUENT user-defined-functions, Three-dimensional.

Introduction

Very few studies have involved full numerical simulations of filtration combustion. Most of these studies have been limited to a counter-flow or co-current systems. There are certain limitations in the counter/co-current configurations, which makes it unsuitable for large scale industrial production. The length of the reaction is limited as it controls the length of the filtration path. Hence, high pressures are required to maintain a reasonable pressure gradient to drive the flow of gaseous reactants. At low pressures, pore closures, due to volumetric expansion/sintering, will prevent conversion of the inner layers of the solid. Taking these drawbacks into account, a cross-flow configuration was first proposed by Kumar *et al.* [3]. This configuration is shown in Fig. 1. Gas accessibility to the combustion front significantly improves in the cross-flow configuration due to the transport of the gaseous reactants from the surroundings by a longitudinal flow from above as well as a transverse flow the front. As a result, the combustion synthesis reaction can be completed at low pressures compared to the counter-current configuration. Furthermore, this configuration uses a reactor open at the top, which facilitates product removal.

Calculations for cross-flow filtration combustion in 2-D have been presented for the first time by Dandekar *et al.* [4]. In their study, the results in terms of the effects of pressure, bed height, and porosity were discussed and compared with experimental data.

In this study, we develop a three-dimensional model for the cross-flow configuration, which can offer an understanding of the basic engineering aspects of the behavior of real combustion synthesis systems.

Simulations in Three Dimensions

A two-dimensional model of filtration combustion in FLUENT using user-defined-functions (UDFs) was successfully expanded into the third-dimension to study the behavior of real systems. The UDFs, which are already given by Shim *et al.* [1], will not be repeated here.

The principle aim of three dimensional simulations was to verify the validity of use of the two-dimensional approach for simulating filtration combustion in a cross-

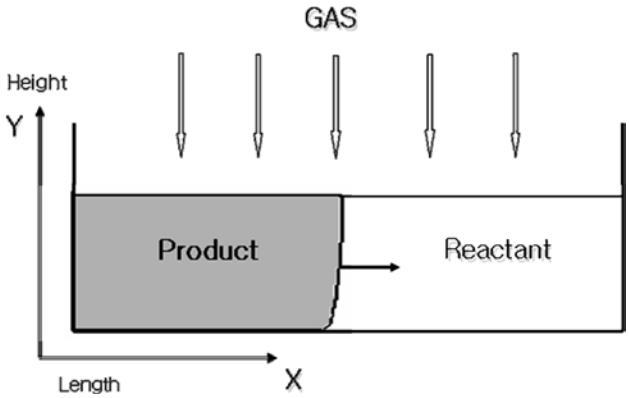

Fig. 1. Cross-flow filtration combustion configuration.

*Corresponding author:
Tel :+82-2-2220-0481
Fax:+82-2-2298-5147
E-mail: scyi@hanyang.ac.kr

flow configuration. A very important aspect of these simulation results was the presentation of the data in graphical form or as visualizations. Given the fact that the data was four dimensional, (parameters as a function of three space variables, varying in time), normal methods of portrayal such as carpet plots and contours were unsuitable. Indeed preliminary representation of the data in the form of surface contours, which involved drawing the contours only on the faces of a rectangular parallelepiped, gave erroneous conclusions. Fig. 2 shows such an attempt. Looking at the contours on the top surface one would be beguiled into believing that there is indeed no variation along the Z direction. However, as results discussed later show, there is considerable variation along the Z direction.

Example

The UDFs described above [1] were successfully used for simulation of the filtration combustion process for the synthesis of nitrides. An important subclass of materials prepared by a self-propagating high-temperature synthesis (SHS) process is made up of substances that result from the reaction between a porous solid sample and a gaseous reactant. As a result, several hydrides and nitrides have been experimentally obtained [5, 6].

SHS is an efficient method where combustion waves are employed to synthesize the desired high-temperature materials. Using an ignition wire or hot plate, the reactive system is ignited locally. At high temperature, the solid particles react with the gaseous oxidizer to form a solid product. Because the chemical reaction is highly exothermic, it can sustain itself, and after a short while the ignition source can be turned off. A luminous region appears, indicating the location of the reaction zone. This zone, under the right conditions, can travel the distance of the system, leaving behind the desired refractory product. The process is self-propagating, meaning no additional external energy needs to be provided. Please refer to Dandekar *et al.* [4] for additional information on the filtration combustion process.

In terms of the dimensionless variables which are standard in the combustion literature[7, 8], the governing equations for a three-dimensional description of the physical system may be written as follows:

mass balance in the gas phase :

$$\frac{\partial(\alpha\bar{\varepsilon}\bar{\rho}_g)}{\partial\bar{t}}=\frac{\partial(\alpha\bar{\varepsilon}\bar{\rho}_g\bar{\upsilon}_x)}{\partial\bar{x}}-\frac{\partial(\alpha\bar{\varepsilon}\bar{\rho}_g\bar{\upsilon}_y)}{\partial\bar{y}}-\frac{\partial(\alpha\bar{\varepsilon}\bar{\rho}_g\bar{\upsilon}_y)}{\partial\bar{z}}-\gamma^{-1}R \tag{1}$$

heat balance the system :

$$\frac{\partial(\alpha\delta_1\bar{\varepsilon}\bar{\rho}_g+1-\eta+\delta_2\delta\eta)\theta}{\partial\bar{t}}=\frac{\partial}{\partial\bar{x}}\left(\bar{\lambda}\frac{\partial\theta}{\partial\bar{x}}\right)+\frac{\partial}{\partial\bar{y}}\left(\bar{\lambda}\frac{\partial\theta}{\partial\bar{y}}\right)$$

$$+\frac{\partial}{\partial\bar{z}}\left(\bar{\lambda}+\frac{\partial\theta}{\partial\bar{z}}\right)-\frac{\partial(\alpha\delta_1\bar{\varepsilon}\bar{\rho}_g\bar{\upsilon}_x\theta)}{\partial\bar{x}}-\frac{\partial(\alpha\delta_1\bar{\varepsilon}\bar{\rho}_g\bar{\upsilon}_y\theta)}{\partial\bar{y}}$$

$$-\frac{\partial(\alpha\delta_1\bar{\varepsilon}\bar{\rho}_g\bar{\upsilon}_z\theta)}{\partial\bar{z}}+[(1+\delta_1-\delta_2)(\beta\gamma)^{-1}+\gamma^{-2}]R \tag{2}$$

equation of state :

$$\pi=\frac{\bar{\rho}_g(1+\beta\theta)}{(1+\beta\theta_0)} \tag{3}$$

Darcy's law :

$$\bar{\upsilon}_x=-\omega\frac{\partial\pi}{\partial\bar{x}}\quad\bar{\upsilon}_y=-\omega\frac{\partial\pi}{\partial\bar{y}}\quad\bar{\upsilon}_z=-\omega\frac{\partial\pi}{\partial\bar{z}} \tag{4}$$

reaction rate expression :

$$\frac{\partial\eta}{\partial\bar{t}}=\gamma^{-1}(1-\eta)exp\left(\frac{\theta}{1+\beta\theta}\right)\pi=\gamma^{-1}R \tag{5}$$

The parameters β and γ appear almost everywhere in studies on strongly exothermic reaction systems with a high activation energy. They represent the inverse of the dimensionless activation energy and the inverse of the dimensionless temperature rise, respectively. Parameter a specifies the ratio of the amount of gaseous reactant initially present inside the system to the amount of gas necessary to bring the reaction to full conversion. A low gas pressure therefore corresponds to $\alpha << 1$ and a high gas pressure to $\alpha \approx 1$. The permeability of a porous solid structure is measured by parameter ω. When ω is large, the gas velocity will far exceed the reaction front

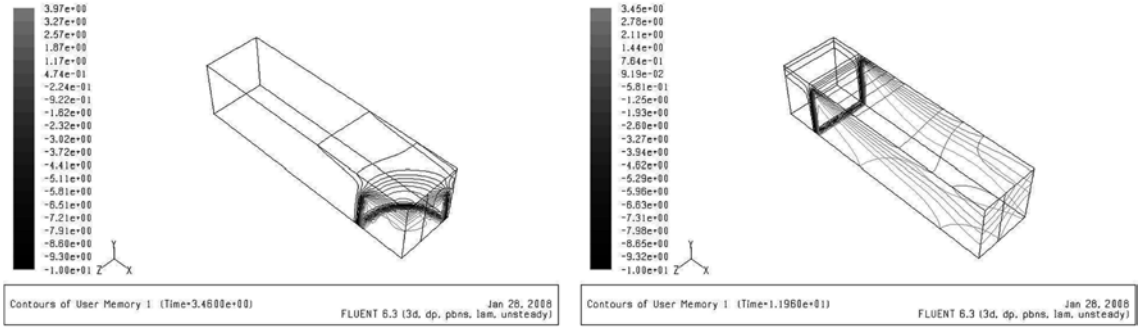

Fig. 2. Surface contour representation of front propagation in three dimensions; $L_x = 20$, $L_y = 5$, $L_z = 5$, $\alpha = 1.0$, $\gamma = 0.05$, $\beta = 0.08$, a) $\bar{t} = 3.46$, b) $\bar{t} = 11.96$.

propagation velocity, whereas for a small ω the permeability of the system is very low and the gas mobility is accordingly much less. The heat capacity ratios are given by δ_1 and δ_2. For simplicity, it can be assumed that $\delta_2 = 1 + \delta_1$. The form for the dependence of the reaction rate on the conversion was chosen since the reaction rate depends much more strongly on temperature due to the high value of the activation energy.

To complete the formulation of the problem, initial and boundary conditions have to be specified in the system. In a dimensionless form, they can be written as:

initial conditions :

for $\bar{t} = 0$ and $0 \le \bar{x} \le \bar{L}_x$, $0 \le \bar{y} \le \bar{L}_y$, $0 \le \bar{z} \le \bar{L}_z$

$$\begin{array}{ll} \theta = \theta_0 & \eta = 0 \\ \bar{\rho}_g = 1 & \pi = 1 \\ \bar{\upsilon}_x = 0 & \bar{\upsilon}_y = 0 \end{array} \tag{6}$$

boundary conditions :

for $\bar{t}_H > \bar{t} > 0$ and

$\bar{x} = 0 \quad 0 \le \bar{y} \le \bar{L}_y \quad 0 \le \bar{z} \le \bar{L}_z$

$q = q1(x, z) \quad \bar{\upsilon}_x = 0$ (7)

for $\bar{t} > \bar{t}_H$ and

$\bar{x} = 0 \quad 0 \le \bar{y} \le \bar{L}_y \quad 0 \le \bar{z} \le \bar{L}_z$

$$-\bar{\lambda}\frac{\partial\theta}{\partial\bar{x}} = \bar{h}_c(\theta - \theta_0) \quad \bar{\upsilon}_x = 0 \tag{8}$$

$\bar{x} = \bar{L}_x \quad 0 \le \bar{y} \le \bar{L}_y \quad 0 \le \bar{z} \le \bar{L}_z$

$$-\bar{\lambda}\frac{\partial\theta}{\partial\bar{x}} = \bar{h}_c(\theta - \theta_0) \quad \bar{\upsilon}_x = 0 \tag{9}$$

$\bar{y} = 0 \quad 0 \le \bar{x} \le \bar{L}_x \quad 0 \le \bar{z} \le \bar{L}_z$

$$-\bar{\lambda}\frac{\partial\theta}{\partial\bar{y}} = \bar{h}_c(\theta - \theta_0) \quad \bar{\upsilon}_y = 0 \tag{10}$$

$\bar{y} = \bar{L}_y \quad 0 \le \bar{x} \le \bar{L}_x \quad 0 \le \bar{z} \le \bar{L}_z$

$$-\bar{\lambda}\frac{\partial\theta}{\partial\bar{y}} = a\delta_1\bar{\upsilon}_x[(\bar{\varepsilon}\bar{\rho}_g\theta)_0 - (\bar{\varepsilon}\bar{\rho}_g\theta)] + \bar{h}_c(\theta - \theta_0)$$
$$+\bar{h}_r(\theta - \theta_0) \quad \pi = 1 \tag{11}$$

$\bar{z} = 0 \quad 0 \le \bar{x} \le \bar{L}_x \quad 0 \le \bar{y} \le \bar{L}_y$

$$-\bar{\lambda}\frac{\partial\theta}{\partial\bar{z}} = \bar{h}_c(\theta - \theta_0) \quad \bar{\upsilon}_z = 0 \tag{12}$$

$\bar{z} = \bar{L}_z \quad 0 \le \bar{x} \le \bar{L}_x \quad 0 \le \bar{y} \le \bar{L}_y$

$$-\bar{\lambda}\frac{\partial\theta}{\partial\bar{z}} = \bar{h}_c(\theta - \theta_0) \quad \bar{\upsilon}_z = 0 \tag{13}$$

These boundary conditions imply a non-adabatic system with convective heat losses from all sides. Radiative heat losses are accounted for only at the ignition plane. Heat loss from the system to the surroundings can take place both by radiation and natural convection.

Ignition by thermal energy sources takes place at $\bar{x} = L_x$, where the wall is also impermeable to gas penetration. The wall is partially heated to a temperature $\theta_i(x,z)$ for a period of time $\bar{t}_H$, which is of the order of few seconds. The value θ_i is typically the adiabatic temperature of the reaction. The top of the system at $\bar{y} = L_y$ is open to the surroundings and the system can thus freely take up additional gaseous oxidezer under the right conditions.

In particular, an alternative formulation of the mathematical model is employed which substitutes the mass balance in the gas phase with a pressure evolution equation, obtained through a combination of Eqns. (1), (3), and (4):

$$\frac{\partial\left(\alpha\bar{\varepsilon}\left(\frac{1+\beta\theta_0}{1+\beta\theta}\right)\pi\right)}{\partial\bar{t}} = \nabla\cdot\left(\alpha\bar{\varepsilon}\omega\left(\frac{1+\beta\theta_0}{1+\beta\theta}\right)\pi\nabla\pi\right) - \gamma^{-1}R \tag{14}$$

In Fig. 3 contour plots of temperature across z planes are shown at different times after ignition. This system is characterized by the dimensionless parameters $\alpha = 1.0$, $\beta = 0.08$, $\gamma = 0.05$, $\delta_1 = 1.0$, $\delta_2 = 2.0$, $\omega = 30.0$, $\theta_i = 0.0$, and $\theta_0 = -10.0$. Similar plots are presented for pressure and conversion as well in Figs. 4 and 5, respectively. The velocity vector plot for gas flow is shown in Fig. 6.

Combustion front propagation in Figs 3 to 6 show some unique phenomena which justify the need for three dimensional simulations. As shown there are hot spots formed along the width of the reactor. Thus there is seen a considerable variation of temperature along the direction of the width. From the animation, the unfurling and rolling back behavior of the cylinder shape hot spot can be conjectured much like a flag which then rolls back again into a cylinder from the animation prepared in the FLUENT. This unfurling and rolling takes place along the width of the boat, as the front propagates along the length. These phenomena would have remained undiscovered in the absence of three dimensional simulations. It is very difficult to obtain experimental verification of these results since it is next to impossible to measure the high temperatures encountered under these conditions.

It is interesting to observe that the conversion and temperature contours across cross-sections essentially show very little variation after ignition when a staple front propagation is established.

Conclusions

It was shown that FLUENT simulations using user-defined-functions (UDFs) can provide a very powerful tool for the solution of problems involving combustion phenomena. The new three-dimensional model of filtration combustion in FLUENT enhances the capability for design

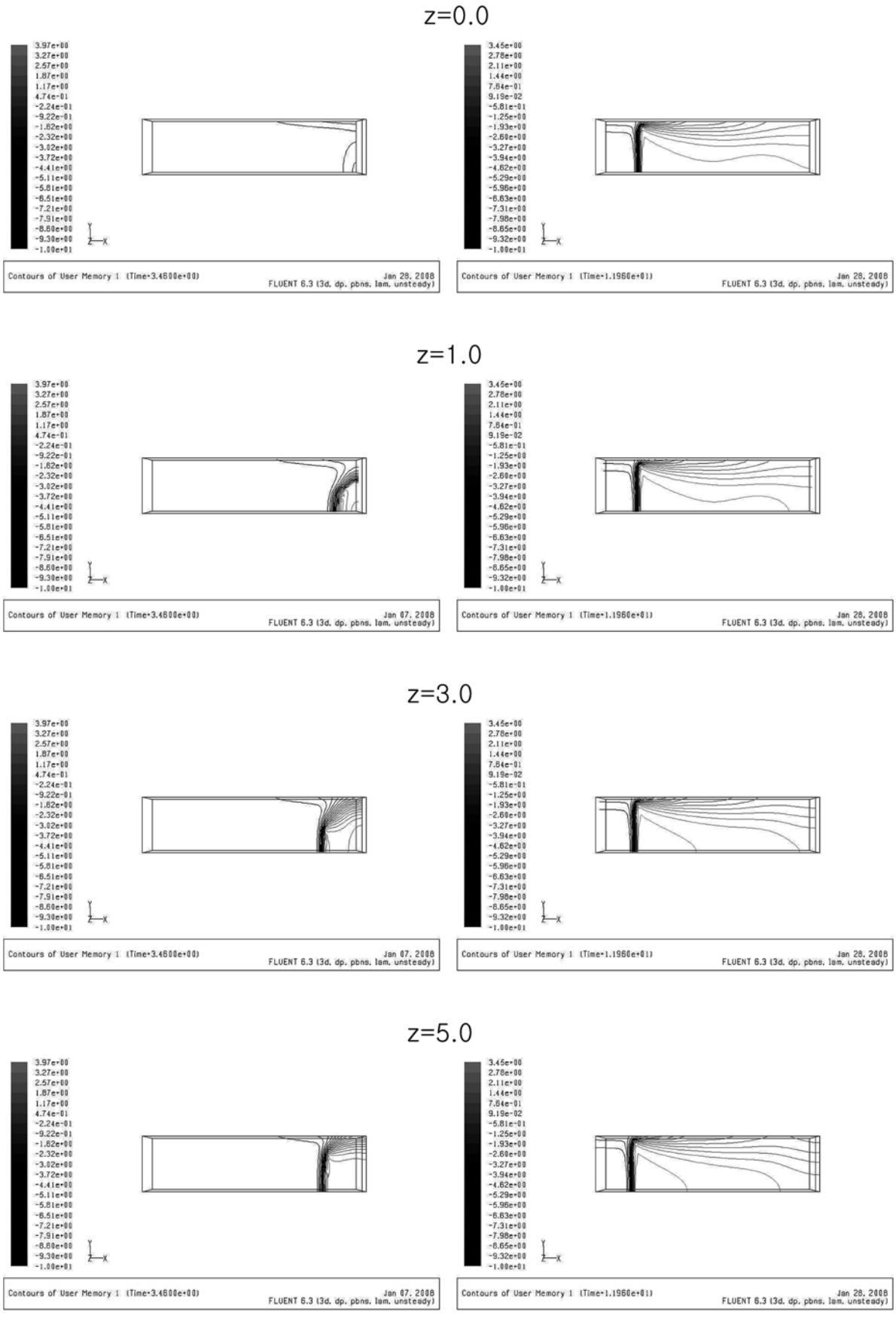

Fig. 3. Contours of temperature across z planes at different times; $L_x = 20$, $L_y = 5$, $L_z = 5$, $\alpha = 1.0$, $\gamma = 0.05$, $\beta = 0.08$, (a) $\bar{t} = 3.46$, (b) $\bar{t} = 11.96$.

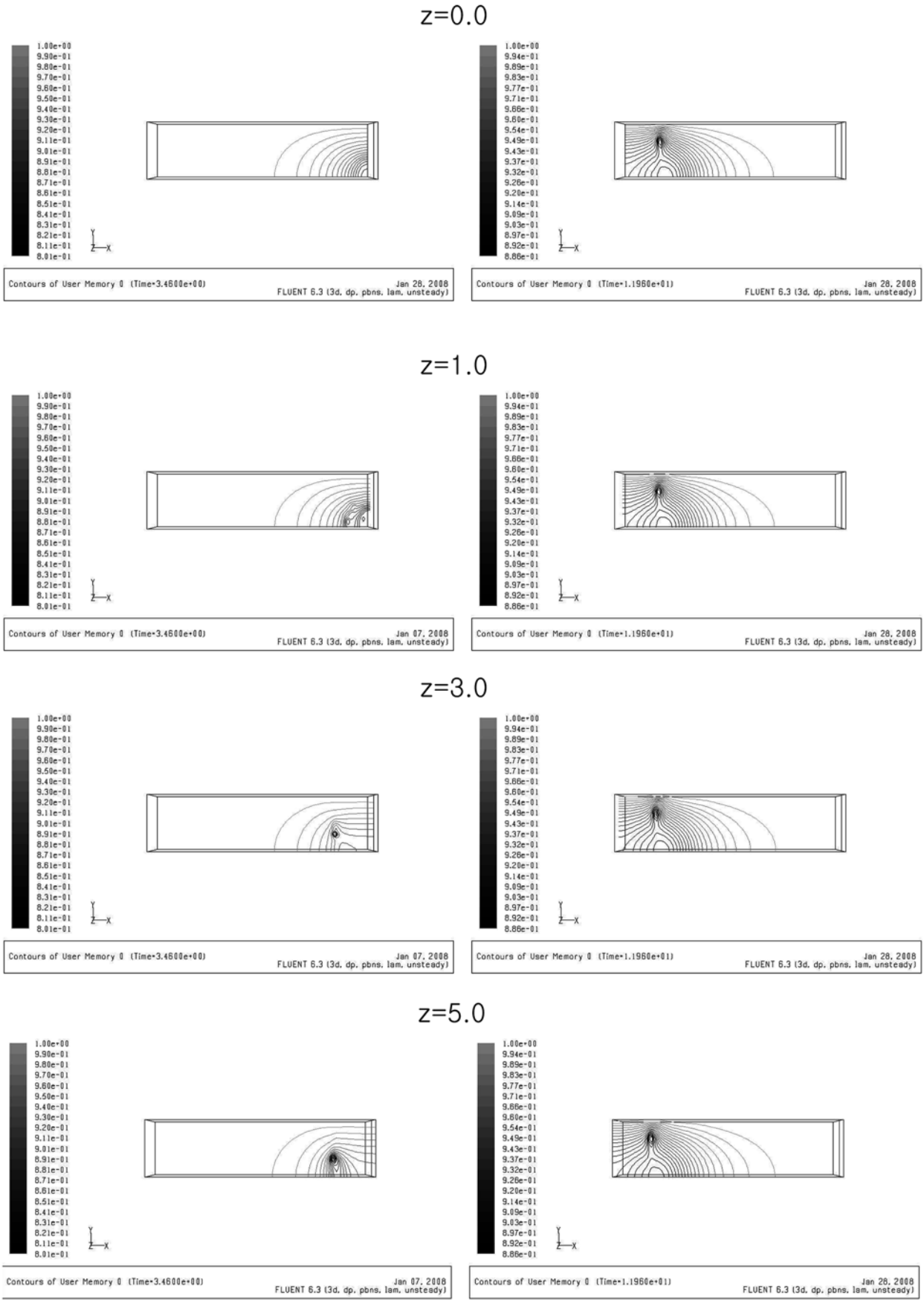

Fig. 4. Contours of pressure across z planes at different times; $L_x = 20$, $L_y = 5$, $L_z = 5$, $\alpha = 1.0$, $\gamma = 0.05$, $\beta = 0.08$, (a) $\bar{t} = 3.46$, (b) $\bar{t} = 11.96$.

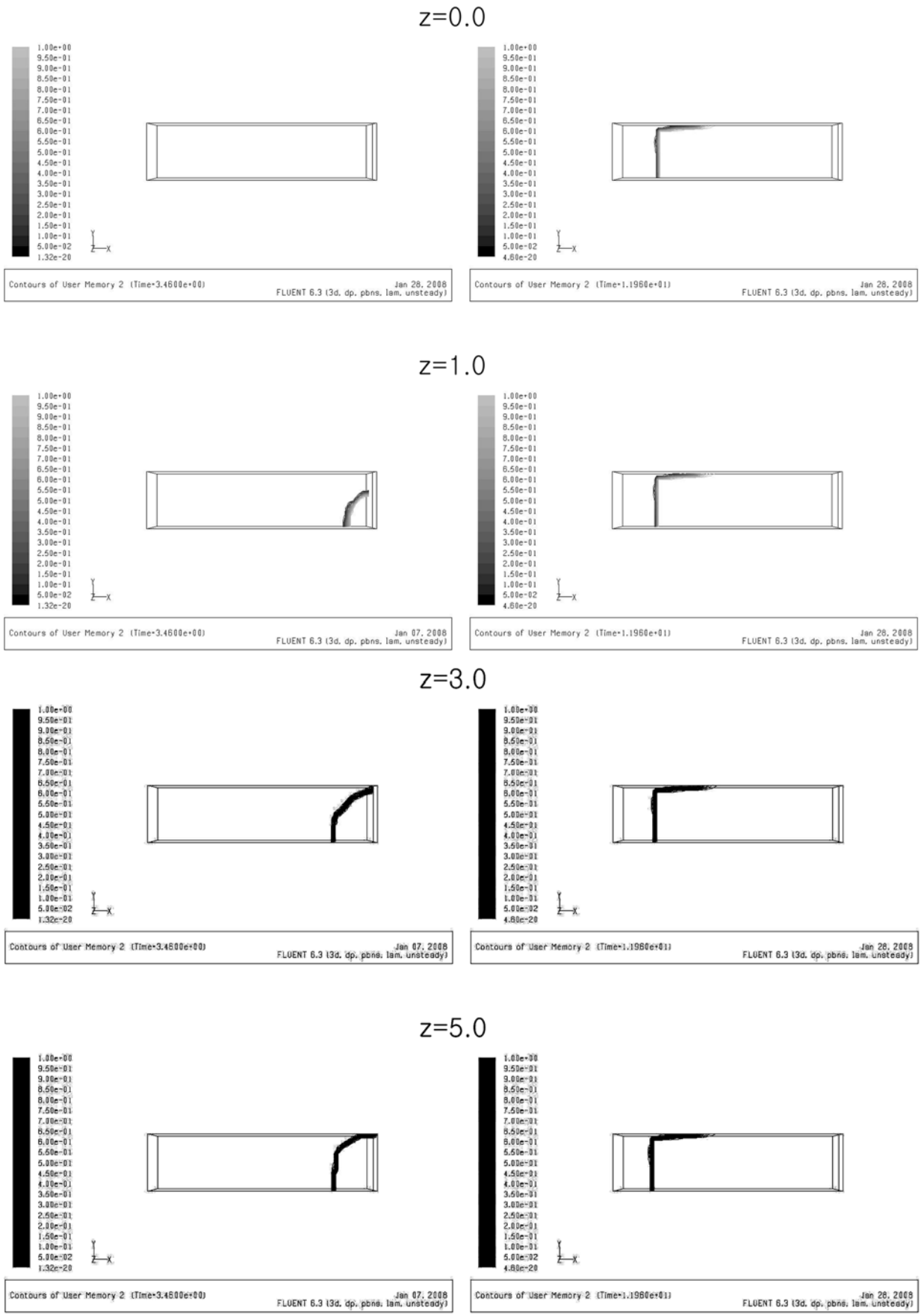

Fig. 5. Contours of conversion across z planes at different times; $L_x = 20$, $L_y = 5$, $L_z = 5$, $\alpha = 1.0$, $\gamma = 0.05$, $\beta = 0.08$, (a) $\bar{t} = 3.46$, (b) $\bar{t} = 11.96$..

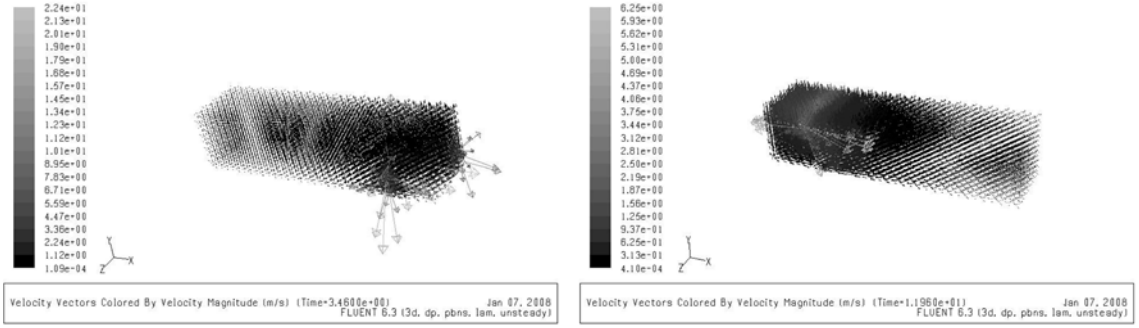

Fig. 6. Gas velocity vector plot in three dimensions at different times; $L_x = 20$, $L_y = 5$, $L_z = 5$, $\alpha = 1.0$, $\gamma = 0.05$, $\beta = 0.08$, (a) $\bar{t} = 3.46$, (b) $\bar{t} = 11.96$

engineers to analyze and optimize the SHS of nitrides.

Although the model developed in this study is robust, many changes can be incorporated into the model as well, such as melting of the solid reactants, chemical reactions ocurring in parallel or in series and structural transformations. For filtration combustion, the propagation characteristics of the combustion front, due to the addition of an inert gaseous species to the gaseous oxidizer, could be considered as a more accurate representation of fluid flow through a reactive porous medium.

Nomenclature

$\bar{L}$	dimensionless length
$\bar{h}_c$	dimensionless convective heat transfer coefficient
$\bar{h}_r$	dimensionless radiative heat transfer coefficient
$\bar{t}$	dimensionless time
$\bar{x},\bar{y}$	dimensionless length coordinate
$\bar{v}$	dimensionless velocity
α	measure of amount of stoichiometric gas in void
β	dimensionless activation energy
γ	dimensionless heat of reaction
δ	ratio of specific heats
ε	void fraction
$\bar{\lambda}$	void fraction
μ	effective thermal conductivity
ϖ	stoichiometric coefficient
η	partial conversion of solid
ω	dimensionless permeability coefficient

Acknowledgement

This research was supported by Hanyang Fusion Materials Program funded by Ministry of Education, Science and Technology, Korea.

Also, it is partially supported by the Manpower Development Program for Energy & Resources supported by the Ministry of Knowledge and Economy (MKE), Republic of Korea.

References

1. K.B. Shim, Y.C. Chung, and S.C. Yi, JCPR, 8 (2007) 364-368.
2. J. Degreve, P. Dimitriou, J. Puszynski, and V. Hlavacek, Comput. Chem. Eng, 11 (1987) 749-755.
3. S. Kumar, C.C. Agrafiotis, J. Puszynski, and V. Hlavacek, AIChE symposium Series, 263 (1988) pp 50.
4. H.W. Dandekar, J. Puszynski, and V. Hlavacek, AIChE Journal, 36 (1990) 1649-1660.
5. A.G. Aleksanyan and S.K. Dolukhanyan, International Journal of Hydrogen Energy, 26 (2001) 429-433.
6. Rosenband, Valery and Alon Gany, Experimental Thermal and Fluid Science, 31 (2007) 461-467.
7. A.G. Merzhanov, A.K. Filonenko and I.P. Borovinskaya, Dokl. Akad. Nauk SSSR 208 (1973) 122-125.
8. A.D. Merzhanov and I. P. Borovinskaya, Comb. Sci. Tech, 10 (1975) 195-211.